

Computations of the Ground State Cohesive Properties Of AlAs Crystalline Structure Using Fhi-Aims Code

G.S.M. Galadanci¹, Garba Babaji²

^{1,2}(Department of Physics, Bayero University, Kano P.M.B. 3011, Kano Nigeria.)

Abstract: A density functional theory codes FHI-aims is used to investigate the material properties of AlAs bulk crystalline structures. The code has several input parameters or variables some of which should be optimized. In the FHI-aims code we study different phases of AlAs crystalline structure and the ground state cohesive properties of the most stable structure of AlAs was computed within GGA and LDA of the density-functional theory. The results of computations shows that the ground state equilibrium properties of and AlAs such as Lattice constants, cohesive energies and Bulk modulus are in agreement with experimentally found values within reasonable percentage errors.

Keywords: bcc, bcc, bulk modulus, cohesive energy, crystalline structure, DFT, fcc, ground state, lattice-constant, simple cubic, and total energy.

I. Introduction

Total Energy calculation and molecular dynamic simulation employing density-functional theory represent a reliable tool in condensed matter physics, material science, and physical chemistry. A large variety of applications such as in molecules, bulk materials and surfaces have proven the power of these methods in analyzing as well as predicting non-equilibrium and equilibrium properties.

Density-functional theory (DFT) is one of the most popular and successful quantum mechanical approaches to matter. It is nowadays routinely applied for computations of ground state properties of molecules and solids such as the binding energy of molecules and the band structure of solids in physics.

This is a computational material science research work in which the ground state properties of AlAs crystals were investigated using DFT based code FHI-aims as a tool. The equilibrium cohesive properties of AlAs crystal were calculated using FHI-aims code.

The program FHI-aims uses DFT as a main production technique to determine electronic and structural properties of molecular or solid condensed matter in its ground state within the local or semi-local approximations[1]. FHI-aims code works on a Linux based operating system in which a FORTRAN-95 or later compiler was installed. A compiled version of lapack libraries and a library providing optimized linear algebra subroutines(BLAS) must also be installed. When the above requirements were made, the FHI-aims executable binary file could then be build. Execution of FHI-aims program requires two input files control.in and geometry.in. The input file contains all the information related to atomic structure and runtime-specific for a given calculation.

This research work was initiated due to the importance of AlAs in the modern technology. Some of the noble importance of AlAs are:

AlAs is a group III/V binary compound semiconductor. AlAs is a compound of aluminum and arsenic. The crystals of AlAs is technologically important and among the most studied compounds semiconductor material. It is used in the manufacture of devices such as microwave frequency integrated circuits, monolithic microwave integrated circuits, infrared light-emitting diodes, laser diodes, solar cells and optical windows[2, 3](Streetman and Banerjee, 2006; Madelung and Landolt-Börnstein, 1982).

Some electronic properties of aluminum arsenide are superior to those of silicon. AlAs has a higher saturated electron velocity and higher electron mobility, allowing its transistors to function at frequencies in excess of 250 GHz. Unlike silicon junctions, AlAs devices are relatively insensitive to heat owing to its wider band-gap. Also, AlAs devices tend to have less noise than silicon devices, especially at high frequencies. This is as a result of higher carrier mobility and lower resistive device parasitics due to radiation. These properties recommend AlAs circuitry in mobile phones, satellite communications, microwave point-to-point links and higher frequency radar systems. It is used in the manufacture of Gunn diodes for generation of microwaves.

AlAs have indirect bandgap and so is very poor at emitting light. Nonetheless, recent advances may make silicon and AlAs LEDs and lasers possible.

As a wide direct band gap material with resulting resistance to radiation damage, AlAs is an excellent material for space electronics and optical windows in high power applications. Combined with the high dielectric constant, this property makes AlAs very good electrical substrate and unlike Si provides natural isolation between devices and circuits. This has made those materials ideal for microwave and millimeter wave

integrated circuits(MMICs), where active and essential passive components can readily be produced on a single slice of AIAs.

With increasing demand for material with wider applications in science and technology and that AIAs crystal is found to be good candidate, there is a need to further study this materials from different perspective. The structural and ground state cohesive properties of this material are studied using FHI-aims codes.

The diamond lattice structure is very common in semiconductor materials, such as Si and Ge. AIAs, GaAs and GaP has a zinblende lattice structure which is similar to the diamond lattice structure. The diamond and zinblende structures are similar except that in diamond structure there is only one type of atom(see Fig.1a.) whereas in zinblende there are two types of atoms. In the AIAs unit cell there are four Al-atoms and the rest are As-atoms(see Fig.1.b.).

Calculation of the bulk ground state properties, such as lattice constants, bulk modulus, cohesive energy, and atomic positions, play an important role in the physics of condensed matter [4. 5]Jappor, 2011; Wachowicz and Kiejna, 2001]. Bulk calculations help us to understand, characterize, and predict mechanical properties of materials in surroundings, under extreme conditions[6] (Hashim *et al*, 2007).

The cohesive energy of crystalline solid structure is defined as the energy that must be added to the crystal to separate its components into neutral free atoms at rest at infinite separation, with the same electronic configuration[7] (Fuchs *et at*, 2002). The term lattice energy is used in discussion of ionic crystals and is defined as the energy that must be added to the crystal to separate its component ions into free ions at rest at infinite separation[2] (Streetman and Banerjee, 2006).

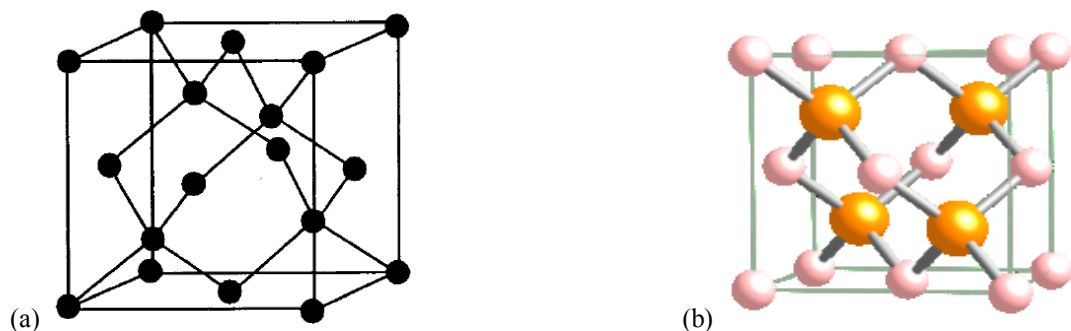


Fig 1. Unit cell structure of (a) Diamond cubic cell and (b) zinblende (AIAs) lattice. Al atoms are shown small, As atoms shown large, and the gray-dashed lines show the unit cell.

1.2 Density Functional Theory

Density Functional Theory (DFT) is a quantum mechanical technique used in Physics and chemistry to investigate the structural and electronic properties of many body systems. DFT has proved to be highly successful in describing structural and electronic properties in a vast class of materials, ranging from atoms and molecules to simple crystals and complex extended systems (including gasses and liquids). Furthermore DFT is computationally very simple. For these reasons DFT has become a common tool in first-principles calculations aimed at describing – or even predicting – properties of molecular and condensed matter systems[8, 9, 10](Giannozzi, 2005; Fiohais *et al*, 2003; Parr and Yang, 1989).

Traditional methods in electronic structure theory, in particular Hartree-Fock theory and its descendents are based on the complicated many-electron wavefunction. The main objective of density functional theory is to replace the many-body electronic wavefunction with the electronic density as the basis quantity. Whereas the many-body wave function is dependent on 3N variables, three special variables for each of the N electrons, the density is only a function of three variables and is a simpler quantity to deal with both conceptually and practically.

Consider a system of N interacting (spinless) electrons under an external potential V (r) (usually the Coulomb potential of the nuclei). If the system has a nondegenerate ground state, it is obvious that there is only one ground-state charge density n(r) that corresponds to a given V(r). In 1964 Hohenberg and Kohn demonstrated the opposite, far less obvious result: there is only one external potential V(r) that yields a given ground-state charge density n(r). The demonstration is very simple and uses a *reductio ad absurdum* argument.

For many-electron Hamiltonian $H = T + U + V$, with ground state Wavefunction, Ψ . T is the kinetic energy, U the electron-electron interaction, V the external potential. The charge density n(r) as defined by Hohenberg and Kohn in 1964 is

$$n(r) = N \int |\Psi(r, r_2, r_3, \dots, r_N)|^2 dr_2 \dots dr_N \quad (1)$$

Considering a different Hamiltonian $H' = T' + U' + V'$ (V and V' do not differ simply by a constant: $V - V' \neq \text{const.}$), with ground state wavefunction Ψ' . Assuming that the ground state charge densities are the same: $n[V] = n'[V']$. Then the following inequality holds:

$$E = \langle \psi' | H' | \psi' \rangle < \langle \psi | H' | \psi \rangle = \langle \psi | H + V' - V | \psi \rangle \quad (2)$$

That is

$$E' < E + \int (V(r) - V'(r))n(r)dx \quad (3)$$

The inequality is strict because Ψ and Ψ' are different, being eigenstates of different Hamiltonians. By reversing the primed and unprimed quantities, one obtains an absurd result. This demonstrates that no two different potentials can have the same charge density.

The first Hohenberg and Kohn (HK) theorem demonstrate the existence of a one-to-one mapping between the ground state electron density and the ground state wavefunction of a many-perticle system. The second Hohenberg and Kohn theorem demonstrate that the ground state density minimizes the total electronic energy of the system. Originally HK theorems held for the ground state in the absence of magnetic field, although they have since been generalized.

A straightforward consequence of the first Hohenberg and Kohn theorem is that *the ground state energy E is also uniquely determined by the ground-state charge density*. In mathematical terms E is a functional, $E[n(r)]$. We can write

$$E[n(r)] = \langle \psi | T + U + V | \psi \rangle = \langle \psi | T + U | \psi \rangle + \langle \psi | V | \psi \rangle = F[n(r)] + \int n(r)V(r)dr \quad (4)$$

where $F[n(r)]$ is a universal functional of the charge density $n(r)$ (and not of $V(r)$). For this functional a variational principle holds: the ground-state energy is minimized by the ground-state charge density. In this way, DFT exactly reduces the N-body problem to the determination of a 3-dimensional function $n(r)$ which minimizes a functional $E[n(r)]$. Unfortunately this is of little use as $F[n(r)]$ is not known.

In 1965, Kohn and Sham (KS) reformulated the problem in a more familiar form and opened the way to practical applications of DFT[11, 12, 13](Burke and Friends, 2008; Martin, 2004; Kratzer *et al*, 1999). The system of interacting electrons is mapped on to an auxiliary system of non-interacting electrons having the same ground state charge density $n(r)$. For a system of non-interacting electrons the ground-state charge density is representable as a sum over one-electron orbitals (the KS orbitals) $\psi_i(r)$ [12,14] (Martin, 2004; Da Silva *et al*, 2006):

$$n(r) = 2 \sum_i |\psi_i(r)|^2 \quad (5)$$

where i runs from 1 to $N/2$ by assuming double occupancy of all states, and the KS orbitals are the solutions of the Schrödinger equation

$$\left(-\frac{\hbar^2}{2m} \nabla^2 + V_{KS}(r) \right) \psi_i(r) = \epsilon_i \psi_i(r) \quad (6)$$

The existence of a unique potential $V_{KS}(r)$ having $n(r)$ as its ground state charge density is a consequence of the Hohenberg and Kohn theorem, which holds irrespective of the form of the electron-electron interaction U .

The problem is now to determine $V_{KS}(r)$ for a given $n(r)$. This problem is solved by considering the variational property of the energy. For an arbitrary variation of the $\psi_i(r)$, the variation of E must vanish. This translates into the condition that the functional derivative with respect to the ψ_i of the constrained functional.

$$E' = E - \sum_{ij} \lambda_{ij} \left(\int \psi_i^*(r) \psi_j(r) dr - \delta_{ij} \right), \quad (7)$$

where the Lagrange multipliers, λ_{ij} must vanish[15, 16](Scheffler, 2001; Taura, 2009):

$$\frac{\partial E'}{\partial \psi_i^*(r)} = \frac{\partial E'}{\partial \psi_i(r)} = 0 \quad (8)$$

It is convenient to rewrite the energy functional as follows:

$$E = T[n(r)] + E_H[n(r)] + E_{xc}[n(r)] + \int n(r)V(r)dr \quad (9)$$

The first term is the kinetic energy of non-interacting electrons. The second term (called the Hartree energy) contains the electrostatic interactions between clouds of charge. The third term, called the exchange-correlation energy, contains all the remaining terms. The logic behind such procedure is to subtract out easily computable terms which account for a large fraction of the total energy. Finally

$$\left(-\frac{\hbar^2}{2m} \nabla^2 + V_H(r) + V_{xc}[n(r)] + V(r) \right) \psi_i(r) = \sum_j \lambda_{ij} \psi_j(r) \quad (10)$$

where V_H is introduced as the Hartree potential, and an exchange-correlation potential, V_{xc} .

2.2 Local Density And Generalized Gradient Approximations

A great variety of different approximations to V_{xc} have been developed. Those approximations are (i) Local Density Approximation, LDA, (ii) Generalized Gradient Approximation, GGA and (iii) Hybrid Approximation. For many years the local density approximation (LDA) has been used [13, 17, 18] (Kratzer *et*

al, 1999; Qing-Miao *et al*, 2007; Juarez *et al*, 2008). In the LDA the exchange correlation energy density at a point in space is taken to be that of the homogeneous electron gas with the local electron density, $\epsilon_{xc}(\mathbf{n})$. Thus the total exchange correlation energy functional is approximated as,

$$E_{xc}^{LDA} = \int n(\vec{r}) \epsilon_{xc}(n(\vec{r})) d\vec{r} \quad (11)$$

from which the potential is obtained as,

$$V_{xc} = \frac{\delta E_{xc}}{\delta n} \quad (12)$$

For many years properties such as structure, vibrational frequencies, elastic moduli and phase stability are described very reliably for many systems. However, in computing energy differences between rather different structures the LDA can have significant errors[14](Da Silva *et al*, 2006). For instance, the binding energy of many systems is overestimated and energy barriers in diffusion or chemical reactions may be too small or absent. Currently, effective potentials that depend both on the local density and the magnitude of its local gradient called, generalised gradient functionals are widely used [19](Ceder and Marzari, 2005). The GGA approach in its various forms goes some way to correcting the problems seen in LDA calculations.

Solids are stable structures, and therefore there exist interactions holding atoms in a crystal together. For example a crystal of sodium chloride is more stable than a collection of free Na and Cl atoms. This implies that the Na and Cl atoms attract each other, i.e. there exist an attractive interatomic force, which holds the atoms together[20](Hans-eric, 2012). This also implies that the energy of the crystal is lower than the energy of the free atoms. The amount of energy which is required to pull the crystal apart into a set of free atoms is called the cohesive energy of the crystal.

$$\text{Cohesive energy} = \text{energy of free atoms} - \text{crystal energy} \quad (13)$$

Magnitude of the cohesive energy varies for different solids from 1 to 10 eV/atom, except inert gases in which the cohesive energy is of the order of 0.1eV/atom [21](Kittel, 1996). The cohesive energy controls the melting temperature .

Calculation of the bulk ground state properties, such as lattice constants, bulk modulus, cohesive energy, and atomic positions, play an important role in the physics of condensed matter[5] [Wachowicz and Kiejna, 2001], bulk calculations help us to understand, characterize, and predict mechanical properties of materials in surroundings, under extreme conditions.

II. Methodology

2.0 FHI-aims Code

FHI-aims(“Fritz Haber Institute ab-initio molecular simulations”) is a computer program package for computational materials science based on quantum-mechanical first principles. The main production method is density functional theory (DFT) to compute the total energy and derived quantities of molecular or solid condensed matter in its electronic ground state. In addition, FHI-aims allows to describe electronic single-quasiparticle excitations in molecules using defferent self-energy formalisms, and wave-function based molecular total energy calculation based on Hartree-Fock and many-body perturbation theory (Blum *et al*, 2009).

The focus here is on density-functional theory (DFT) in the local and semi-local (generalized gradient) approximations, but an extension to hybrid functionals, Hartree–Fock theory, and MP2/*GW* electron self-energies for total energies and excited states is possible within the same underlying algorithms. An all-electron/full-potential treatment that is both computationally efficient and accurate is achieved for periodic and cluster geometries on equal footing, including relaxation and *ab initio* molecular dynamics[22] (Havu *et al* 2009). The construction of transferable, hierarchical basis sets is demonstrated, allowing the calculation to range from qualitative tight-binding like accuracy to meV-level total energy convergence with the basis set. Together with a scalar-relativistic treatment, the basis sets provide access to all elements from light to heavy. Both low-communication parallelization of all real-space grid based algorithms and a ScaLapack-based, customized handling of the linear algebra for all matrix operations are possible, guaranteeing efficient scaling (CPU time and memory) up to massively parallel computer systems with thousands of CPUs [22]((Havu *et al* 2009)

To compute the ground state cohesive properties of AlAs crystal structure, we first calculate the ground state total energies of the most stable structure of AlAs as a function of its lattice constants. The energies are then converted to the cohesive energies as a function of its molecular volumes using the equations[6,23] (Hashim *et al* 2007 and Wieferin *et al*. 2011)

$$E_{coh} = -\frac{E_{bulk} - NE_{atom}}{N} = -\left[\frac{E_{bulk}}{N} - E_{atom}\right] \quad (6)$$

The equilibrium quantities such as the lattice constant a_0 , the cohesive energy E_{coh} , molecular volume, V_0 , the bulk modulus B_0 and its derivative with respect to pressure B'_0 can be obtained by use a thermodynamically

motivated and more accurate fitting function, the Birch-Murnaghan equation of states[23] (Wieferin et al 2011) given by

$$E(V) = E_0 + \frac{B_0 V}{B'_0} \left[\frac{(V_0/V)^{B'_0}}{B'_0 - 1} + 1 \right] - \frac{B_0 V_0}{B'_0 - 1} \quad (7)$$

2.1 General Computational Requirement

All calculations were carried out using fhi-aims code upgrade 5 (released on 17th July, 2011; version 071711_5). It only works on any Linux based operating system. Computations can only be carried out after building an executable binary file. Since the fhi-aims package is distributed in a source code form,

- a. A working Linux-based operating system (Ubuntu 11.10 in this case)
- b. A working FORTRAN 95 (or later) compiler. In this case we use x86 type computer and therefore intel's ifort compiler (specifically Composerxe 2011.6.233) was installed for this work.
- c. A compiled version of lapack library, and a library providing optimized linier algebra subroutines (BLAS). Standard libraries such as Intel's mkl or IBM's essl provide both lapack and BLAS support. Intel's composerxe 2011.6.233 comes with mkl.

All necessary adjustment were made for building the executable binary file for running the code and the executable program was successfully build.

FHI-aims requires two input files: (1). **control.in**:- which contains all runtime-specific informations and (2). **geometry.in**:- which contains information directly related to the atomic structure for a given calculation. The two input files must be places in the same directly from where the FHI-aims binary file is invoked at the terminal.

2.2 Constructions of the Input Files and Running the FHI-aims Code

Our first step towards studying periodic systems with FHI-aims is to construct periodic geometries in the FHI-aims geometry input format (geometry.in). Next, we set basic parameters in control.in for periodic calculations. Finally, we compare total energies of different AIs bulk geometries.

A **geometry.in** files for the AIs bcc and zinc-blende structures were constructed using the experimental lattice constants a of 5.3 Å for bcc and 5.6 Å for zincblende.

In setting up the **geometry.in** file of a periodic structure in FHI-aims all three lattice vectors as well as the atomic positions in the unit cell must be specified. The lattice vectors are specified by the keyword `lattice_vector`. For example, bcc AIs with a lattice constant a in Å is defined as

```
lattice_vector    -a/2    a/2    a/2
lattice_vector    a/2    -a/2    a/2
lattice_vector    a/2    a/2    -a/2
atom    0.0    0.0    0.0 Al
atom    a/4    a/4    a/4 As
```

Similarly zinc-blende AIs with a lattice constant a in Å is defined as

```
lattice_vector    -0.0    a/2    a/2
lattice_vector    a/2    0.0    a/2
lattice_vector    a/2    a/2    0.0
atom    0.0    0.0    0.0 Al
atom    a/4    a/4    a/4 As
```

A **control.in** input files for AIs was created with the following settings.

```
# Physical settings
xc    pw - lda
spin    none
relativistic atomic_zora scalar
# SCF settings
charge_mix_param    0.2
n_max_pulay    8
sc_accuracy_eev    1E-2
sc_accuracy_etot    1E-5
sc_accuracy_rho    1E-4
sc_iter_limit    40
# k - grid settings
k_grid    3 3 3 (to be adjusted)
```

Additionally, the default “light” species settings for Al and As as supplied with the code: **species_defaults/light/31_Al_default** and **species_defaults/light/33_As_default**.

A bash script named **run.sh** was created to calculate total energies of the different phases of AIAs as a function of lattice constant a . For this, seven different values of a in steps 0.1 Å around the lattice constants given above was used for each structure.

Note that the grid factors refer to the reciprocal lattice vectors corresponding to the real-space lattice vectors in **geometry.in**. If there are inequivalent lattice vectors, their order in **geometry.in** determines the ordering of reciprocal lattice vectors in the code.

The total energy per atom of each structure was plotted as a function of the lattice constant using origin. From the plot the most stable structure was determined.

2.3 Energy Convergence Tests

Here we will explicitly check total energy convergence for zincblende AIAs with respect to the k-grid and to the basis set. One directory was dedicate for every series of these calculations.

2.3.1 k-grid convergence test

The total energies for zinc-blende AIAs was calculated as a function of the lattice constant for k-grids of $8 \times 8 \times 8$, $10 \times 10 \times 10$, $12 \times 12 \times 12$, and $16 \times 16 \times 16$. The same computational settings and the same lattice constants as in the previous calculations of section 2.1 was used. A graph of all the total energies and another with the computational times drawn against lattice constant were plotted. The results of $3 \times 3 \times 3$ from previous runs was added. From the plots the k-grid for which the AIAs zinc-blende is most stable with minimal energy was found.

2.3.2 Convergence With Basis Set Size

The total energies for zincblende AIAs as a function of the lattice constant for the minimal and the tier1 basis sets were calculated. The same lattice constants and computational settings as in 2.2 together with the $10 \times 10 \times 10$ k-grid were used. Again, one plot with the total energies and another with the computational times were drawn. The results for the minimal+spd basis set were obtained from the k-point convergence test above and added to the results. The basis size settings was changed by looking into the species-dependent settings within control.in. There, there exist a line starting with “# "First tier" - ...”. Each line after this defines a basis function which is added to the minimal basis. Right now, there is one additional function for each valence function (s and p) as well as a d function to allow the atoms to polarize. This is what we call minimal+spd in the context of this work. In quantum chemistry and in particular the Gaussian community, this type of basis set is often called “double zeta (ζ) plus polarisation” (DZP). Again from the plot the basis set for which the AIAs zincblende structure gives the minimal energy and minimal convergence time was determined.

2.4 Phase Stability and Cohesive Properties

After finding “converged” computational settings, we now revisit the phase stability of bulk AIAs. Note that in practice convergence must be achieved first in order to avoid false conclusions. We will now compute the basic cohesive properties and study the pressure dependence of phase stability.

2.4.1 Recalculation of $E(a)$ curves

The total energies of bcc AIAs as a function of lattice constant a are calculated. The settings from section 2.3 (k-grid of $10 \times 10 \times 10$, minimal+spd basis) and the same lattice constants as in section 2.1 were used. The results obtained and that of zincblende AIAs obtained in section 2.3 were plotted as in section 2.2 and the plots were analyzed to ascertain the most stable phase of AIAs crystal.

2.4.2 Calculations of Cohesive energies and atomic volumes

The total energy of a free atom for AIAs unit cell zincblende is calculated as follows: For the single atom energy, special care has to be taken. First, the free atom is of course spin polarized and we use “**spin collinear**” instead of “spin none” as well as properly initialize the magnetization with “**default_initial_moment hund**”. Second, we use a more converged basis. In particular, we use all basis functions up to “tier 3”, the cutting potential was increase to “**cut_pot 8. 3. 1.**”, and basis dependent confining potentials was turned off with “**basis_dep_cutoff 0**”

The cohesive energy (E_{coh}) of a crystal is the energy per atom needed to separate it into its constituent atoms. E_{coh} is defined as

$$E_{coh} = -\frac{E_{bulk} - NE_{atom}}{N} = -\left[\frac{E_{bulk}}{N} - E_{atom}\right] \quad (6)$$

where E_{bulk} is the bulk total energy per unit cell and N the number of atoms in the unit cell. E_{atom} is the energy of the isolated atom calculated above.

In order to compare the pressure dependence of phase stabilities we need to express the lattice constant behavior of all phases on equal footing. One possibility to do so is to express the lattice constant in terms of the volume per atom. This atomic volume can be calculated quite easily from the lattice constant a . The simple cubic (super-)cell has the volume $V_{\text{sc}} = a^3$. This number has to be divided by the number of atoms N_{sc} in this cell $V_{\text{atom}} = a^3/N_{\text{sc}}$. Note that there are two, and eight atoms in the simple cubic supercell in the case of the *bcc*, and the zincblende structure, respectively.

A file *energy.dat* containing the lattice constants and total energies per atom was converted to a file *cohesive.dat* containing atomic volumes V_{atom} and (negative) cohesive energies $-E_{\text{coh}}$ by the use of the script *convert-coh.awk* which is provided in the code.

2.4.3 Calculation of cohesive properties at equilibrium.

An important equilibrium quantity we can calculate from our data is the equilibrium lattice constant a_0 . In principle, this can be done with a quadratic ansatz for $E(a)$ or $E(V)$. Here we use a thermodynamically motivated and more accurate fitting function, the Birch-Murnaghan equation of states[22]. The energy per atom ($E = -E_{\text{coh}}$) is expressed as a function of the atomic volume ($V = V_{\text{atom}}$) as in equation (7).

The cohesive energy data for the zincblende phase of AIAs calculated above was fitted to the Birch-Murnaghan equation of states using the program *murn.py*. The lattice constant a , the bulk modulus B_0 , and the cohesive energy per atom E_{coh} at equilibrium are determined. The calculated cohesive properties in this work are compared with the experimental values and those determined in other theoretical works.

2.5 Convergence Test and Calculations of Cohesive Properties Using fine-tuned Lattice constants.

From the plots of section 2.2 the lattice constant that give the minimum total energy was determined for both *bcc* and zincblende AIAs crystal structure up to four decimal places of accuracy. The same was repeated for the k-grids of 8x8x8, 10x10x10, 12x12x12 and 16x16x16 of zincblende structure. The FHI-aims was run to calculate the total energies for, seven different values of a in steps 0.0001 Å around the lattice constants found above for each structure. The resultant k-grid was used to carried out the basis convergence test as in section 2.2. The result obtained for the basis convergence was used to calculate the cohesive properties such as V_0 , the equilibrium molecular volume, E_0 , the molecular energy, the equilibrium lattice constant a_0 , the bulk modulus, B_0 and B'_0 derivative with respect to pressure of bulk modulus as in section 2.3.2.

III. Results

3.0 Introduction

The output files of the computations were use to deduce the tables of lattice constants against the total energies and graphs were plotted to obtain the optimized parameters for AIAs structures within both LDA and GGA. The optimized parameters were then used to obtained the equilibrium ground state properties of AIAs crystalline structure.

3.1 Graphical Representation of Data

The following graphs summarize the output data obtained during the convergence test, and are used in obtaining the optimized values of the parameters investigated.

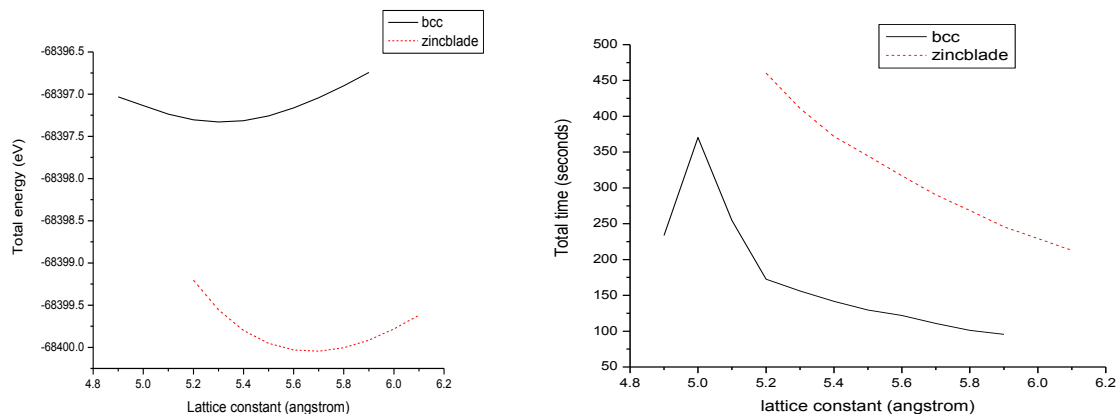
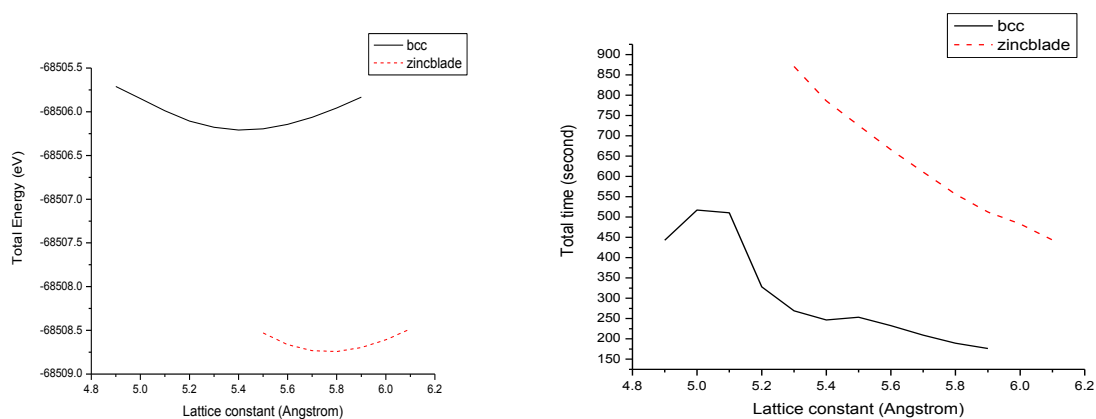
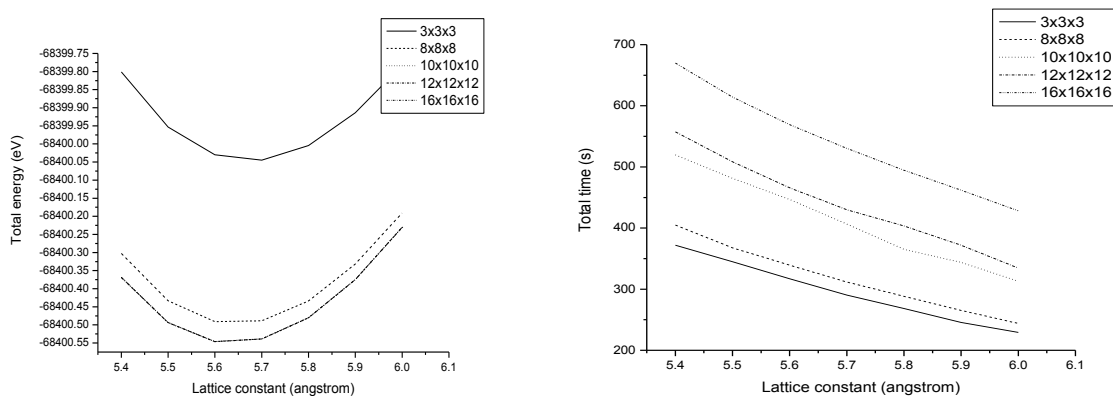


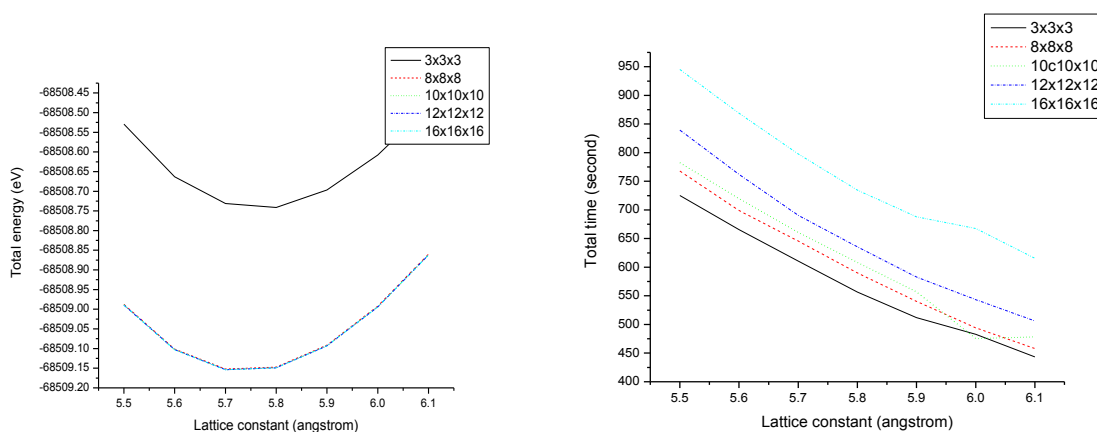
Fig.2. Plots of Total Energy (a) and Total time (b) against Lattice constant for bcc and zincblende AIAs structure within LDA XC- functional



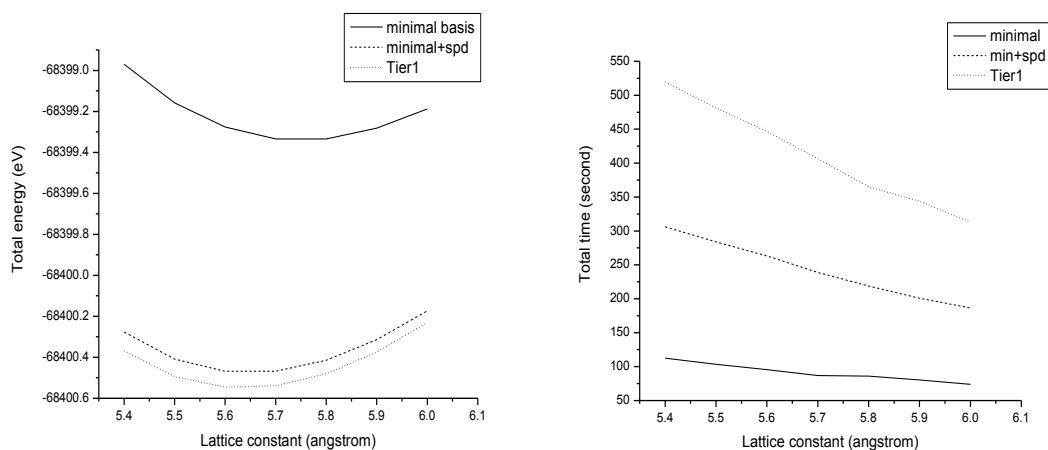
(a) (b)
Fig.3. Plots of Total Energy (a) and Total time (b) against Lattice constant for bcc and zincblende AlAs structure within GGA XC-functional



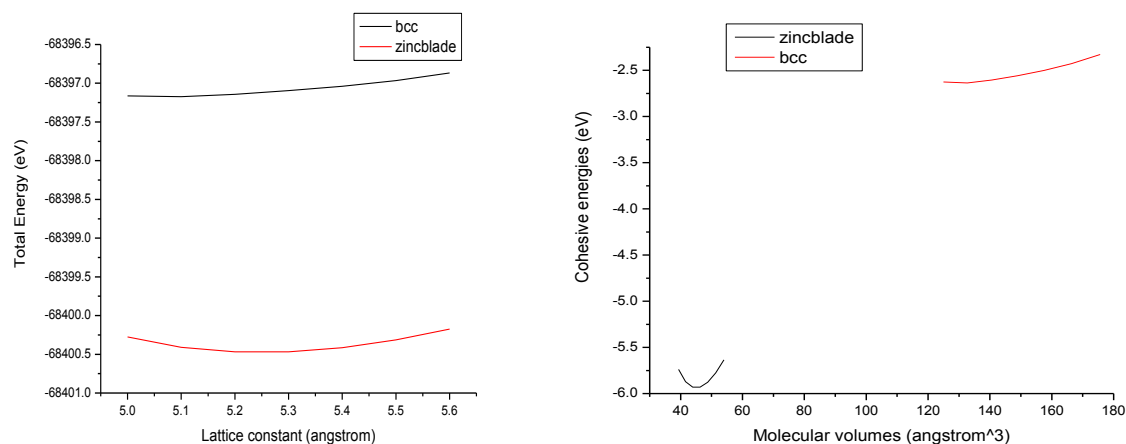
(a) (b)
Fig. 4. Plots of (a) Energies and (b) total times against lattice-constants for various kgrids of AlAs zinc-blende structure within LDA.



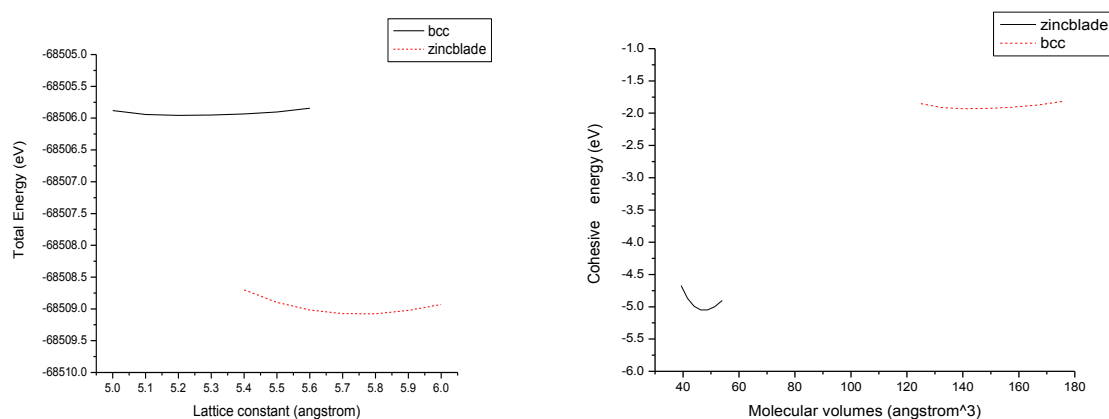
(a) (b)
Fig. 5. Plots of (a) Energies and (b) total times against lattice-constants for various kgrids of AlAs zincblende structure within GGA.



(a) (b)
Fig.6. Plots of (a) total energies and (b) total time against lattice constant for three different basis of AlAs zincblende crystal within LDA.



(a) (b)
Fig.7. Plots of (a) total energies versus lattice-constant and (b) cohesive energies versus molecular volumes of bcc and zincblende structures of AlAs within LDA XC-functional



(a) (b)
Fig.8. Plots of (a) total energies versus lattice-constants and (b) cohesive energies versus molecular volumes of bcc and zincblende structures of AlAs within GGA XC-functional.

3.2 Tabular Representation Results

TABLE 1: List of Minimum Total Energy and Total Time Against Lattice Constant for Determination of the Most Stable Phase of AlAs Structure.

Phase	XC	Lattice-constant (Å ^o)	E _{min} (eV)	Total time (s)
BCC	LDA	5.3	- 68397.3297389759	156.213
	GGA	5.4	- 68506.2096932378	246.766
ZINCBLEND	LDA	5.7	- 68400.0447821083	290.259
	GGA	5.8	-68508.7410032641	556.509

TABLE 2: Cohesive Properties of AlAs Zincblend Crystal

Property	Present using GGA xc	Present using LDA xc	Experimental	Others
Lattice constant (Å ^o)	5.749542362	5.647908525	5.662[24](Sayed <i>et al</i> , 1984)	5.661[25](Powel, 2007)
Cohesive energy (eV/atom)	-5.0551700666	-5.93731365155	-4.67[26](Verma, 2010)	-5.22[26] (Verma, 2010)
Bulk modulus B ₀ (GPa)	66.340307	71.676059	74.7[24] (Sayed <i>et al</i> , 1984)	78.1[25] (Powel, 2007)
B ₀ '	3.3700769341	3.70687713385	-	-

IV. Discussion

From Fig.2 and 3, it is clear that the zincblende phase of AlAs has much lower total energy than that of bcc phase. Thus zincblende phase is the most stable at ground state and is chosen to be the unit cell of interest in this work as in agreement with the experiment and other theoretical works..

From Fig.4a., it can be seen that, the total energy of AlAs computed for 3x3x3 within LDA gives an error of about 0.501 eV from the most accurate value given by 16x16x16 kgrid. The 8x8x8 kgrid calculations reduced the error to about 55 meV. The 10x10x10 kgrid drastically reduced the error to about 0.29 meV. Furthermore, the 12x12x12 k-grid converges within 0.05 meV. Similarly, from Fig.5a., the total energy of AlAs calculated for 3x3x3 kgrid within GGA converges within 0.41 eV of the most accurate calculation of 16x16x16. The 8x8x8 fixed the error to about 1.6 meV. The 10x10x10 kgrid on the other hand is converged within 0.26 meV. The 12x12x12 reduces the error to about 0.05 meV.

Looking at the computational times for both AlAs LDA and GGA (Fig.4.b and Fig.5.b) calculations, we noticed two general trends in FHI-aims. First, the times strongly decrease towards larger lattice constants. This is because there is less overlap between atoms and so less integrations are needed. The approach of FHI-aims is particularly efficient for “open” structures where the atoms occupy more space and thus have less neighbors. Second, increasing the number of *k*-points does not affect the computational times significantly up to comparably dense *k*-grids. A total energy calculation with a 10×10×10 grid is not so much more expensive than a 3×3×3 calculation. Only with even denser *k*-grids computational times increase become noteworthy. In conclusion, the 10×10×10 *k*-grids was chosen for zincblende phase AlAs as a good compromise of high accuracy and reasonable computational time.

From Fig.6 was generally noticed that, the minimal basis gives completely nonphysical results; there is not even an energetic minimum within the calculated range of lattice constants. The *minimal* basis lacks the flexibility to give reasonable geometries. On the other hand, the binding curve does not change significantly from *minimal+spd* to the full *tier1* basis set whereas the computational effort increases significantly by adding the *f* functions from *minimal+spd* to full *tier1*.

While the total energy difference of 70meV between *minimal+spd* and *tier1* is still larger than what we were aiming for in the case of the *k*-grid, we can make use of the fact that the total energy is variational so that a large part of the basis set error actually cancels nicely in energy differences. Thus the *minimal+spd* basis was as a compromising choice between accuracy and reasonable computational time for AlAs calculation within both LDA and GGA.

The resulting binding curves shown in Fig.7. and Fig.8. show that the experimentally observed zincblende structure of AlAs is moststable in LDA and GGA calculation among the crystal structures studied in this work.

After finding “converged” computational settings, we now revisit the phase stability check of bulk GaAs as in section 3.1 before proceeding to calculate the basic cohesive properties avoid false conclusions. The reresulting binding curves shown in Fig.7 and 8 clearly show that the experimentally observed zincblende structure of AlAs is most stable in LDA and GGA among the crystal structures studied in this work. From the ground state cohesive properties of AlAs obtained as compared with the experimentally obtained values and other theoretically computed results, the lattice-constants obtained is under estimated by about 0.014

A° for LDA and over estimated by about 0.088 angstrom within GGA computations. The error obtained in the calculation of the cohesive energies of AlAs are 1.27 eV for LDA and 0.39 eV for GGA. The bulk-modulus of AlAs computed in this work differ from the experimental values for both LDA and GGA calculations by 3.024 GPa and 8.360 GPa respectively.

V. Conclusion

The ground state cohesive properties such as the lattice constant, cohesive energy and bulk modulus of AlAs zinblende crystal within LDA and GGA were calculated. The values obtained are in agreement with the available theoretical and experimental values reported within some reasonable percentage errors. It could be concluded that, the lattice constant calculated in this work differ from experimentally reported results by 0.25% for LDA and 1.00% for GGA. The calculated cohesive energies for AlAs are observed to be different from the experiment by 8.35% for LDA and 27% for GGA. The bulk modulus computed for AlAs in this work for LDA and GGA are respectively 4.00% and 11.2% below the experimentally reported results.

References

- [1]. Blum, V., Gehrke R, Hanke F, Havu P, Havu V, Ren X, Reuter K, Scheffler M. *Ab initio* molecular simulations with numeric atom-centered orbitals. Computer Physics Communications, 180, 2175-2196, (2009).
- [2] Streetman, B.G., Banerjee, S.K., *Solid State Devices 6th ed.* Pearson Education, Inc, New Jersey, 2006.
- [3] Madelung, O., (ed.), Landolt-Börnstein, *Semiconductor. Physics of II-IV and I-VII Compounds, Semi-magnetic Semiconductors, New Series, Group III, V.17*, Springer, Berlin, 1982.
- [4] Jappor, H.R., *Band-Structure Calculations of GaAs within Semiempirical Large Unit Cell Method* E.J.S.R. Vol.59 No.2 (2011), pp.264-275.
- [5] Wachowicz, E., and Kiejna, A., 2001, "*Bulk and surface properties of hexagonal-close-packed Be and Mg*", J. Phys.: Condens. Matter Vol.13, pp 10767- 10776.
- [6] Hashim, F.S., Jappor, H.R., Al-Ammar, K.H.B., *Structural and electronic properties of gallium arsenide crystal using INDO method* Babylon University, 2007.
- [7] Fuchs, M., Da Silva, J.L.F., Stampfl, C., Neugebauer, J., and Scheffler, M., *Cohesive properties of group-III nitrides: A comparative study of all-electron and pseudopotential calculations using the generalized gradient approximation* (13 pages). Phys. Rev. B **65**, 245212 (2002).
- [8] Giannozzi, P., *Density Functional Theory for Electronic Structure Calculations* Struttura della Materia Vol.1 (2005).
- [9] Fiolhais, C., Nogueira, F., Marques, M., *A Primer in Density Functional Theory*, Springer-Verlag Berlin, 2003.
- [10] Parr R. G., Yang W., *Density Functional Theory of Atoms and Molecules* (Oxford University Press, New York, 1989).
- [11] Burke, K. and Friends, *Basics of DFT* (17th August, 2008). Book available online at <http://chem.ps.uci.edu/kieron/dft/book/>.
- [12] Martin, R.M., *Electronic Structure: Basic Theory and Practical Methods* (Cambridge University Press, 2004).
- [13] Kratzer, P. Morgan, C.G., Penev, E., Rosa, A.L., Schindlmayr, A., Wang, L.G., Zywiets, T., *FHI98MD Computer Code for Density Functional Theory Calculations for Poly-atomic Systems: Users Manual*, Program Version 1:03 (August, 1999).
- [14] Da Silva, J.L.F., Stampfl, C., Scheffler, M., *Converged Properties of Clean Metal Surfaces by All-electron First Principle Calculations*, Surface Science **600** (2006) pp. 703-715. Available at www.sciencedirect.com and www.elsevier.com/locate/susc
- [15] Scheffler M., *Present Status of Ab initio Electronic Structure Calculations*, DFT workshop, FHI-Berlin, July 8 – August 1, 2001.
- [16] Taura L.S., *Total Energy Calculation of Bulk Crystal Using FHI98MD Code*, PhD Thesis, Department of Physics, Bayero University, Kano, 2009.
- [17] Qing-Miao, H, Karsten, R, and Scheffler, M, *Towards an Exact Treatment of Exchange and Correlation in Materials: Application to the "CO Adsorption Puzzle" and Other Systems*, Phys. Rev. Lett. **98**, 176103 (2007).
- [18] Juarez L. F. Da Silva¹, and S. Catherine, *Trends in adsorption of noble gases He, Ne, Ar, Kr, and Xe on Pd₃(111): All-electron density-functional calculations*, PHYSICAL REVIEW B **77**, 045401 (2008)
- [19] Ceder, G., Marzari, N., *Atomic Modelling of Materials: Density Functional Practice* (1st March, 2005), Vol. 3, pp. 320.
- [20] Hans-Erik N., *Crystal structures (A Self study material in Solid State Electronics using Multimedia)*. Available online at <http://www.nts.se/~hasse/solid1.html>. Accessed on 09/02/2012.
- [21] Kittel C. *Introduction to Solid state Physics*, 7th ed., John Wilay and Sons Inc. Newyork, 1996.
- [22] Havu V., Blum V., Havu P., and Scheffler M., *Efficient O(N) integration for all-electron electronic structure calculation using numeric basis functions*. J. Comp. Phys., accepted (August 13, 2009).
- [23] Wieferin, J., Nemeč, L. Blum, V, *Tutorial II: Periodic systems Manuscript for Exercise Problems: Presented at the Hands-on Tutorial Workshop on "Ab initio Molecular Simulations at Fritz-Haber-Institut der Max-Planck-Gesellschaft Berlin, July 14, 2011.*
- [24] Sayed, M., Jefferson, J. H., Walker, A. B. and Cullis, A. G.: Nucl. Instrum. Methods Phys. Res. B **102**, 218 (1995).
- [25] Powell, D., Migliorato, M. A., and Cullis, A. G., *Optimized Tersoff potential parameters for tetrahedrally bonded III-V semiconductors*, PHYSICAL REVIEW B **75**, 115202 (2007)
- [26] Verma, A.S., Sarkar, B.K., and Jindal, V.K.; Cohesive energy of zinblende ($A^{\text{III}}B^{\text{V}}$ and $A^{\text{II}}B^{\text{VI}}$) structured solids, Pramana journal of Physics, Indian Academy of Sciences Vol. 74, No. 5 pp. 851-855, May 2010.